

# Pounding of Seismically Isolated Reinforced Concrete Buildings Subjected to Near-Fault Ground Motions

**D.R. Pant & A.C. Wijeyewickrema**

*Tokyo Institute of Technology, Japan*



## **SUMMARY:**

The influence of seismic pounding on the response of a code-designed four-story base-isolated reinforced concrete (RC) building is investigated. Three-dimensional nonlinear finite element analyses are carried out considering bounding values of isolator properties. Fourteen near-fault ground motions containing strong velocity pulses and representing the maximum considered earthquake are used to explore the effects of pounding with the retaining walls at the base. It is shown that pounding increases the mean inter-story drift by 20%. Dispersions in the peak responses under individual ground motions are higher when pounding is considered compared with the no-pounding case. Significantly larger dispersions are also observed when upper bound values of isolator properties are used compared with lower bound values. Findings of the study are expected to assist the design of base-isolated RC buildings.

*Keywords: Base isolation, near-fault ground motion, nonlinear analysis, seismic pounding*

## **1. INTRODUCTION**

Seismic pounding refers to the collision between adjacent structures during earthquakes, which occurs when structures with different dynamic characteristics, having insufficient separation vibrate out of phase. Although seismic pounding of fixed-base buildings has been studied extensively for more than two decades (see for example Anagnostopoulos 1988 and Karayannis and Favvata 2005), seismic pounding of base-isolated buildings has not drawn much attention, until more recently (see for example Tsai 1997 and Polycarpou and Komodromos 2010). Previous studies indicate that the response of a base-isolated building is substantially influenced by seismic pounding. However, except Tsai (1997) who modeled buildings as elastoplastic shear beams, the other studies have been carried out using simplified multi-degree-of-freedom lumped mass systems, assuming that the superstructure remains elastic. Recently, in the ATC-63 project (FEMA 2009) a methodology was presented to determine the probability of failure given the maximum earthquake. Included in the example applications and supporting studies, is the collapse evaluation of seismically isolated structures considering pounding with retaining walls at the base. Pant and Wijeyewickrema (2012) considered seismic pounding of a 4-story base-isolated reinforced concrete (RC) building with retaining walls at the base and a 4-story fixed-base RC building.

The objective of the present study is to assess the effects of seismic pounding on the structural performance of seismically isolated RC buildings subjected to near-fault ground motions. In particular, seismic pounding of a typical four-story base-isolated RC building with retaining walls at the base was studied. Three-dimensional models with distributed plasticity beam-column elements were used and geometric nonlinearity was considered. A modified Kelvin-Voigt impact force model, which has recently been proposed (Pant et al. 2010) and implemented in an existing finite element program OpenSees (2010), was used to simulate the impact.

## 2. BASE-ISOLATED BUILDING AND FINITE ELEMENT MODELING

A four-story, 3-bay by 3-bay base-isolated RC moment-frame building was chosen as a typical building (Fig. 2.1(a)). The retaining walls located on both sides of the building extend from ground level up to the base level of the building. The bay width of the building in both directions is 6.0 m. The story height of the building is 4.0 m, except for the first story which is 4.5 m high. The building was designed by the equivalent lateral force (ELF) procedure, following the provisions of 2012 International Building Code (ICC 2012), ASCE 7-10 (ASCE 2010), and ACI 318-11 (ACI 2011). The building was assumed to be located on a stiff soil site (Site Class D) and was intended to be used as an office building (risk category II). The mapped Risk-targeted Maximum Considered Earthquake (MCE<sub>R</sub>) spectral response acceleration parameters are  $S_s = 1.609g$  and  $S_1 = 0.593g$  at short periods and 1 s period, respectively. The superstructure of the building was designed for the forces associated with the design earthquake (DE) and the isolation system was designed for the effects of MCE<sub>R</sub>. The compressive strength of concrete is 28 MPa, and the yield strengths of main steel reinforcement bars and ties are 420 MPa and 300 MPa, respectively. Beams and column section details are shown in Table 2.1; the slab thickness is 200 mm. Dead load consists of member self-weight, and 7.6 kN/m and 6.8 kN/m loads due to partitions and external cladding on base beams and floor beams, respectively. Live loads on floor and roof slabs were assumed to be 4.8 kPa and 1.0 kPa, respectively. Total seismic weight  $W = 21,809$  kN. The design base shear coefficient was determined as 0.147. Based on the Site Class, design spectral accelerations, and risk category, seismic design category D was assigned and the special moment frame (SMF) system was chosen for the superstructure. Accidental eccentricity of 5% of the plan dimension of the building was considered in both the directions. The lead rubber bearing (LRB) isolation system was chosen for the building and typical bounding values of isolator properties were considered in design (Pavlou 2005). Identical 650 mm diameter circular bearings having a lead core of 113 mm diameter were provided under each of the sixteen column bases. Each bearing consists of forty seven 5 mm thick rubber layers alternating with 2 mm thick steel shims. The main properties of the isolation system for the DE and MCE<sub>R</sub> based on the lower bound (LB) properties of isolators are shown in Table 2.2.

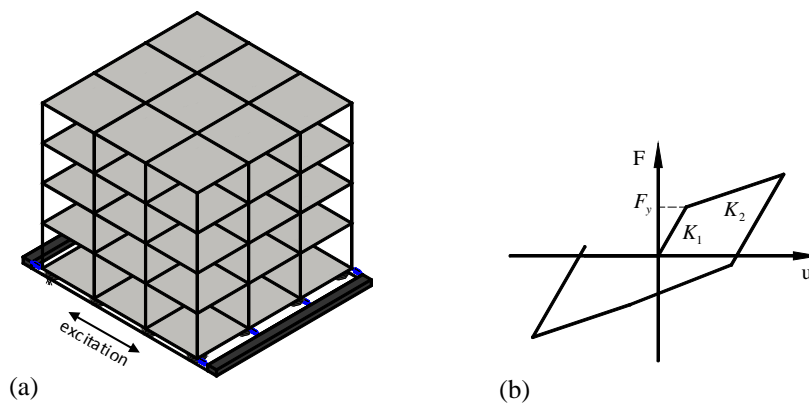


**Fig. 2.1.** (a) Three-dimensional model of the building and (b) bilinear hysteretic force-deformation relationship of isolators.

**Table 2.1.** Section sizes and reinforcement details of the building.

Elements	Size (mm <sup>2</sup> )	Longitudinal reinforcement			Shear reinforcement <sup>a</sup>
		Top	Center	Bottom	
Floor beams	625×625	4 No. 29		4 No. 25	4 legs at 100 mm
Roof beams	625×525	4 No. 19		3 No. 16	2 legs at 95 mm
Columns	625×625	3 No. 32	2 No. 32	3 No. 32	3 legs at 100 mm

<sup>a</sup>No. 10 bar was used as shear reinforcement.

**Table 2.2.** Lead rubber bearing (LRB) isolation system characteristics based on LB isolator properties.

	DE	MCE <sub>R</sub>
Effective period	$T_D = 2.24$ s	$T_M = 2.53$ s
Effective damping	$\beta_D = 27.2\%$	$\beta_M = 18.8\%$
Isolator displacement	$D_D = 201$ mm	$D_M = 383$ mm
Total displacement	$D_{TD} = 231$ mm	$D_{TM} = 440$ mm

Three-dimensional FE model of the building was developed in OpenSees (2010). Beams and columns were modeled using force-based, Euler-Bernoulli fiber beam-column elements that account for the spread of inelasticity along the length of the element. For concrete the modified Kent and Park model (Park et al. 1982) was used in compression and an initial linear elastic branch together with a linear softening branch up to zero stress was used in tension. The model proposed by Yassin (1994) was used to account for concrete damage and hysteresis. For reinforcing steel, the constitutive model of Menegotto and Pinto (1973), which includes strain hardening and the Bauschinger effect, was used. In this study, the strain-hardening ratio is taken as 1%. Lead rubber bearings were modeled using elastomeric bearing elements. A bilinear hysteretic model that is well suited for lead rubber bearings was used to represent the lateral force-deformation relationship of each element (Naeim and Kelly 1999). The values of initial stiffness  $K_1$ , yield force  $F_y$ , and  $\alpha = K_2/K_1$ , where  $K_2$  is the post-elastic stiffness (Fig. 2.1(b)), assigned to the bilinear hysteretic model for each element are shown in Table 2.3.

In-plane stiffness of slabs was accounted for by using rigid truss elements connecting two ends of each beam element and opposite corners of each slab of every bay. Out-of-plane stiffness of slabs was neglected. Accidental eccentricities were not considered in the model. Neglecting the viscous damping in bearings (hysteretic damping being modeled explicitly), 5% stiffness-proportional damping, where damping coefficient was calculated using the fundamental frequency of the entire base-isolated building based on the post-elastic stiffness of the isolation system, was applied only to the superstructure. Impact between the base slab and the retaining walls was modeled using zero-length elements, which were used as contact elements between the base slab and a retaining wall (see Fig. 2.1). The material property of the contact elements was based on the modified Kelvin-Voigt model. The total stiffness of the spring elements between the base slab and a retaining wall, computed as the axial stiffness of the building slab is 5,000 MN/m. The backfill soil-structure interaction was considered outside the scope of this study.

**Table 2.3.** Properties of elastomeric bearing elements.

	Lower bound	Upper bound
Initial stiffness $K_1$ (kN/m)	5945.5	8858.7
Yield force $F_y$ (kN)	111.4	133.7
$\alpha = K_2/K_1$	0.1	0.1

### 3. EARTHQUAKE GROUND MOTIONS

Fault-normal components of 14 near-fault ground motions containing strong velocity pulses were selected from a database of 91 records compiled by Baker (2007) and obtained from Pacific Earthquake Engineering Research Center database (PEER 2011). In the present study the criteria imposed for the selection based on the recommendations of ATC-63 project (Pg. A-8, FEMA 2009) are: (i) magnitude of the earthquake  $M_w \geq 6.5$ ; (ii) peak ground acceleration (PGA) is greater than 0.2g; (iii) source-to-site distance taken as average of the Campbell fault distance and the Joyner-Boore fault distance is less than 10 km; (iv) lowest usable frequency is not greater than 0.167 Hz; (v) record

Site Class is either of B, C, or D; and (vi) instrument was in a free-field condition. For criteria (iv) we have chosen a frequency of 0.167 Hz instead of 0.25 Hz recommended by the ATC-63 project to include the records for the evaluation of base-isolated buildings with periods up to 6 s. Twelve of these records (Table 3.1) are the same as the ones listed in FEMA (2009) *near-field pulse records subset*. As shown in Fig. 3.1, the arithmetic mean of 5%-damped pseudo acceleration and displacement response spectra of ground motions closely match MCE<sub>R</sub>-level design response spectra in a period range of  $0.5T_D$  to  $1.25T_M$  (BSSC 2009, ASCE 2010).

**Table 3.1.** Earthquake ground motions used in the present study.

EQ No.	Record ID	Event (Station)	$M_w$	Year	PGA (g)	PGV (cm/s)	PGD (cm)
1	ELCEN6	Imperial Valley-06 (El Centro Array #6)	6.5	1979	0.44	111.85	66.58
2	ELCEN7	Imperial Valley-06 (El Centro Array #7)	6.5	1979	0.46	108.79	45.55
3	STU	Irpinia, Italy-01 (Sturmo)	6.9	1980	0.23	41.40	22.10
4	PTS	Superstition Hills-02 (Parachute Test Site)	6.5	1987	0.42	106.77	50.70
5	SAA	Loma Prieta (Saratoga - Aloha Ave)	6.9	1989	0.36	55.54	29.41
6	ERZ	Erzican, Turkey (Erzincan)	6.7	1992	0.49	95.40	32.09
7	PET	Cape Mendocino (Petrolia)	7.0	1992	0.61	81.87	25.48
8	LUC	Landers (Lucerne)	7.3	1992	0.72	129.59	137.50
9	RRS	Northridge-01 (Rinaldi Receiving Sta)	6.7	1994	0.87	167.05	28.83
10	SOVMF	Northridge-01 (Sylmar-Olive View Med FF)	6.7	1994	0.73	122.75	31.74
11	TCU065	Chi-Chi, Taiwan (TCU065)	7.6	1999	0.82	127.81	93.27
12	TCU082	Chi-Chi, Taiwan (TCU082)	7.6	1999	0.25	56.11	71.65
13	TCU101	Chi-Chi, Taiwan (TCU101)	7.6	1999	0.22	68.39	71.94
14	TCU102	Chi-Chi, Taiwan (TCU102)	7.6	1999	0.29	106.76	88.00

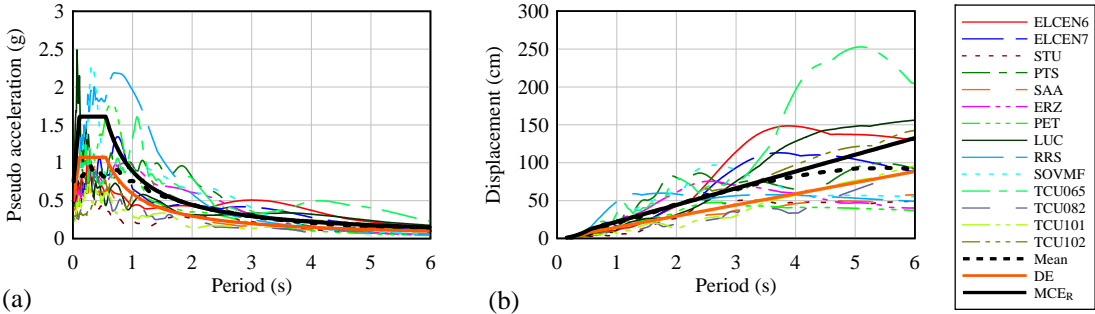


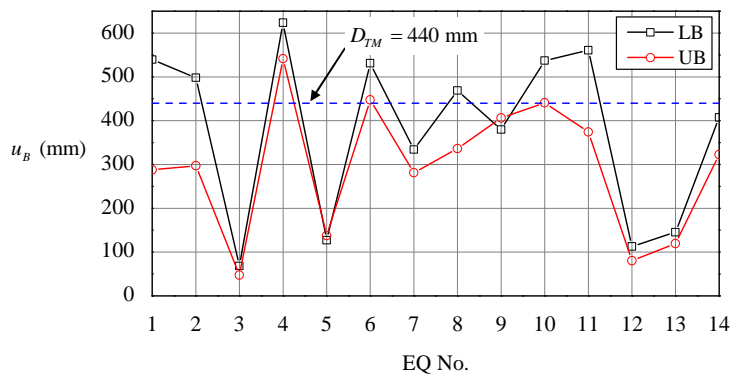
**Fig. 3.1.** Comparison of 5%-damped elastic response spectra of ground motions and their mean with DE- and MCE<sub>R</sub>-level design response spectra: (a) pseudo acceleration and (b) displacement.

#### 4. TIME-HISTORY ANALYSIS RESULTS

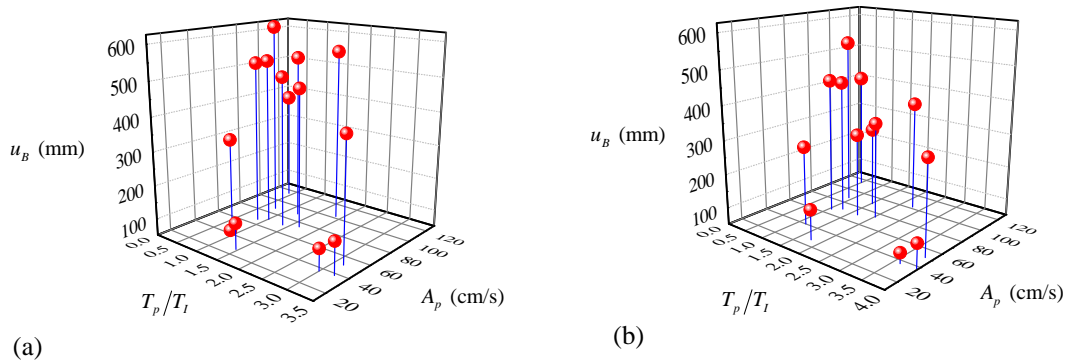
Nonlinear time-history analyses were carried out for the suite of earthquake ground motions applied in the direction as shown in Fig. 2.1(a). The  $P-\Delta$  effects for the superstructure as well as the isolation system were considered in the analyses. The separation distance between the building and retaining walls was set equal to the code-recommended value of  $D_{TM} = 440$  mm (ASCE 2010). Analyses were also performed without considering pounding with the retaining walls at the base. While the main response indicators presented are peak inter-story drift ratio, residual inter-story drift ratio, peak story shear force, and peak column curvature ductility demand, where necessary, peak base displacements are also shown to further explain the building response. Here, story shear forces were normalized by the seismic weight  $W$  and the column curvature ductility demand at a story was evaluated as the peak observed among all the columns of the story. In this study, peak inter-story drift ratios in the ranges of 0.2%–0.5%, 0.5%–1.5%, and 1.5%–3% correspond to only non-structural damage, moderate structural damage, and severe structural damage, respectively (Elnashai and Sarno 2008). Peak inter-story drift ratios greater than 3% can be assumed to correspond to a collapsed story. Statistical distribution of the results is presented in terms of arithmetic mean and 84<sup>th</sup> percentile values (computed as mean plus one standard deviation).

Figure 4.1 shows peak horizontal base displacements  $u_b$  for each ground motion using lower bound (LB) as well as upper bound (UB) properties of isolators when pounding was not considered in the analyses. It is clear from Fig. 4.1 that the displacement demands for several ground motions are greater than  $D_{TM}$ , indicating potential for pounding. Base displacement is plotted against, ratio of pulse period  $T_p$  to the fundamental period of the structure  $T_1$  (computed using post-elastic stiffness of the isolation system) and the amplitude of the pulse  $A_p$  in Fig. 4.2. It is seen that the displacement demand depends greatly on the pulse amplitude in combination with  $T_p/T_1$ . In particular, the records with  $T_p/T_1$  close but somewhat less than unity and with high pulse amplitude were found to be imposing large displacement demands on the isolators. For example, when lower bound properties of isolators are considered, records STU and PTS (see Table 3.1) have  $T_p/T_1$  equal to 1 and 0.7, respectively; however, since PTS has a pulse amplitude of 87.69 cm/s which is more than two times the pulse amplitude of STU; PTS imposes much larger displacement demand of 623.3 mm compared with 68.3 mm imposed by STU.

Figures 4.3 and 4.4 present the mean and 84<sup>th</sup> percentile values of response indicators of the building. The difference between the 84<sup>th</sup> percentile and mean values represents the dispersion (i.e., standard deviation) of responses under individual ground motions from the mean. High dispersion indicates a lesser confidence in predicted response indicators. When pounding was not considered, the mean as well as 84<sup>th</sup> percentile inter-story drift ratios using lower bound model are less than or in the order of



**Fig. 4.1.** Peak horizontal base displacements of the building when pounding was not considered. The dashed line indicates the separation distance  $D_{TM} = 440$  mm.



**Fig. 4.2.** Relationship among peak horizontal base displacement, ratio of pulse period to the period of the building, and pulse amplitude: (a) lower bound and (b) upper bound.

0.5% indicating essentially no structural damage to the building (Fig. 4.3(a)). However, when upper bound model is used, mean inter-story drift ratio at the first story is 0.7% indicating moderate structural damage to the building. The 84<sup>th</sup> percentile inter-story drift ratio at the first story using upper bound model is greater than 1.5% indicating severe structural damage. The difference between lower and upper bound models is more pronounced at lower stories compared with the upper stories. It is also observed that the response of the building using upper bound model is unfavorable as it shows large deviation of the response indicators from the mean compared with the response obtained using lower bound model. Similar trend is also observed in residual inter-story drift ratios, where mean values remain very low at less than 0.05% (Fig. 4.3(b)). The mean values of base shear forces obtained using lower and upper bound models are about  $0.2W$  and  $0.23W$ , respectively Fig. 4.3(c). The deviation in shear force values from the mean is less compared with that observed for inter-story drift ratios. Compatible with inter-story drift ratios are the column curvature ductilities, which show that essentially no yielding occurs (reflected by ductilities of less than or in the order of 1) in any column when lower bound properties of isolators are used (Fig. 4.3(d)). While the mean value of ductility at the first story using upper bound model indicates that minor yielding of the first story columns occurs, the 84<sup>th</sup> percentile value reflects significant yielding of the columns. Trends in the deviations of the ductility demands from the mean are similar to the trends in inter-story drift ratios.

When pounding was considered in the analysis, mean values of inter-story drift ratios at first and second stories using lower bound model are more than 0.5 %, indicating moderate structural damage to the building (Fig. 4.4(a)). Because of pounding, the mean inter-story drift ratios at the first story are increased by a factor of 2.6 and 1.2 using lower and upper bound properties of isolators, respectively. Both lower and upper bound models yield responses with large deviation from the mean. Because of pounding, the 84th percentile inter-story drifts at the first story using lower and upper bound models are increased by a factor of 3.6 and 1.4, respectively. Increase in mean and the 84th percentile values of residual inter-story drift ratios is larger compared with the increase in peak inter-story drift ratios (Fig. 4.4(b)). Increase in mean story shear forces due to pounding is negligible considering the upper bound properties of isolators (Fig. 4.5(c)). However, considering lower bound properties of isolators, the mean and 84th percentile base shear forces are increased by a factor of 1.2 due to pounding. Increase in curvature ductility demands due to pounding is the highest among all response indicators. The mean curvature ductilities at the first story are increased by a factor of 6 and 1.4 using lower and upper bound properties of isolators, respectively (Fig. 4.5(d)). However, the 84th percentile curvature ductilities at the first story are increased by a factor of 8.7 and 1.5 using lower and upper bound properties of isolators, respectively. Interestingly, the mean values of the inter-story drift ratios, story shear forces, and column curvature ductilities are nearly the same using lower and upper bound models; while the mean residual inter-story drift ratios show a very small difference using the two models. This is because the lower bound model tends to increase the base displacement and hence the severity of impact, while upper bound model tends to decrease the base displacement but transfer larger forces to the superstructure. In addition, the effect of seismic pounding is more pronounced in the immediate vicinity of impact (i.e., at the first story).

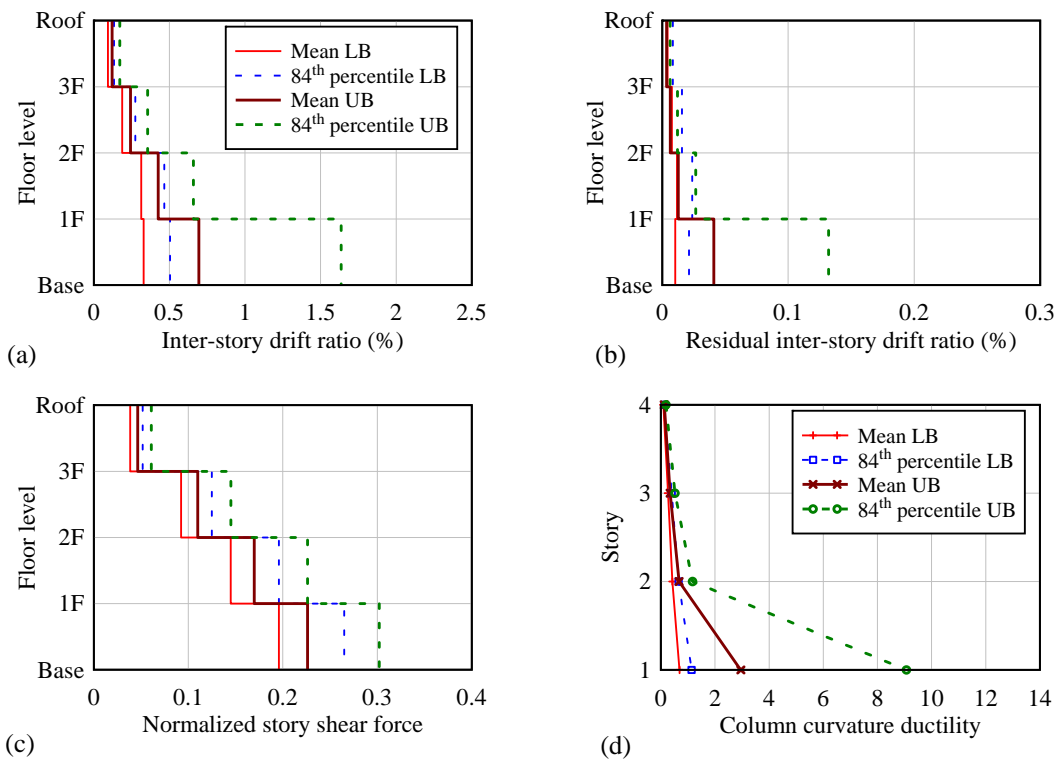


**Fig. 4.3.** Response of the building when pounding is not considered: (a) peak inter-story drift ratio; (b) residual inter-story drift ratio; (c) peak normalized story shear force; and (d) peak column curvature ductility.

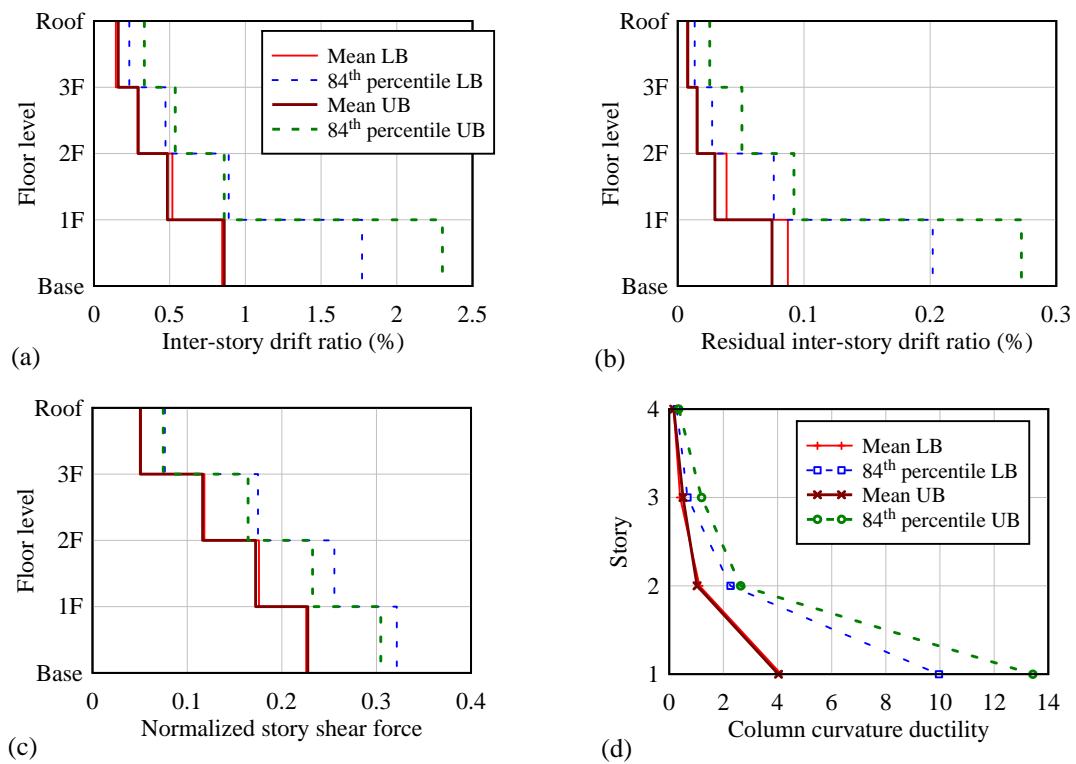


**Fig. 4.4.** Response of the building considering pounding: (a) peak inter-story drift ratio; (b) residual inter-story drift ratio; (c) peak normalized story shear force; and (d) peak column curvature ductility.

Table 4.1 shows maximum response of the base-isolated building at the first story, generated due to all earthquake ground motions. Even though pounding does not occur, the maximum inter-story drift ratio considering upper bound properties of isolators exceeds 3%, indicating collapse of the first story. This is unacceptable for a well-designed base-isolated building, which shows that the response of base-isolated structures is affected strongly by the pulse-like characteristics of near-fault ground motions. Pounding exacerbates the situation leading to a peak inter-story drift ratio of 5.71% and residual inter-story drift ratio of 0.75%.

**Table 4.1.** Maximum values of response indicators at the first story of the building.

	Peak inter-story drift ratio (%)		Residual inter-story drift ratio (%)		Peak normalized story shear force	
	LB	UB	LB	UB	LB	UB
No pounding	0.63	3.81	0.038	0.35	0.29	0.32
Pounding	3.29	5.71	0.34	0.75	0.33	0.32

## 5. CONCLUSIONS

Seismic pounding response of a typical four-story base-isolated RC building was studied using a suite of 14 near-fault pulse-like ground motions. It was shown in this paper that the maximum isolator displacement demands of the building under 7 ground motions exceed  $D_{TM}$ , when lower bound properties of isolators were considered, indicating the potential for pounding with the retaining walls at the base. The earthquake ground motions with  $T_p/T_l$  close but somewhat less than unity and with high pulse amplitude were found to be imposing large displacement demands on the isolators. When pounding was not considered in the analysis, the mean values of response indicators suggest that in the extreme case, the building undergoes moderate structural damage with a peak inter-story drift ratio of 0.7% at the first story. Results also reveal that the response of the building can be predicted with a higher confidence using lower bound properties of isolators compared with the upper bound properties. However, in the extreme case, the maximum values of response indicators show the imminent collapse of the first story. When pounding was considered, it was found that the response of the building cannot be predicted with a higher confidence as it could be done when pounding does not occur. Because of pounding, considering lower bound properties of isolators, the mean values of response indicators were increased by a factor of 2.6, 1.2, and 6 for peak inter-story drift ratio, story shear forces, and column curvature ductilities, respectively. Although the maximum values of response indicators suggest that the collapse is inevitable when pounding occurs, the mean values suggest that the building undergoes moderate structural damage due to pounding.

## ACKNOWLEDGEMENTS

The first author is pleased to acknowledge a Monbukagakusho (Ministry of Education, Culture, Sports, Science and Technology, Japan) scholarship for graduate students. Financial support from Center for Urban Earthquake Engineering (CUEE), Tokyo Institute of Technology is gratefully acknowledged.

## REFERENCES

- ACI (2011). ACI 318-11: Building Code Requirements for Structural Concrete, American Concrete Institute, Farmington Hills, MI.
- ASCE (2010). ASCE 7-10: Minimum design loads for buildings and other structures, American Society of Civil Engineers, Reston, VA.
- Anagnostopoulos, S.A. (1988). Pounding of buildings in series during earthquakes. *Earthquake Engineering and Structural Dynamics* **16**, 443-456.
- Baker, J.W. (2007). Quantitative classification of near-fault ground motions using wavelet analysis. *Bulletin of the Seismological Society of America* **97**:5, 1486-1501.

- BSSC (2009). FEMA-P750: NEHRP recommended seismic provisions for new buildings and other structures, Building Seismic Safety Council, Washington, DC.
- Elnashai, A.S. and Sarno, L.D. (2008). Fundamentals of Earthquake Engineering, Wiley: United Kingdom.
- FEMA (2009). FEMA P695: Quantification of Building Seismic Performance Factors, Federal Emergency Management Agency, Washington, DC.
- ICC (2012). International Building Code, International Code Council, Country Club Hills, IL.
- Karayannis, C.G. and Favvata, M.J. (2005). Earthquake-induced interaction between adjacent reinforced concrete structures with non-equal heights. *Earthquake Engineering and Structural Dynamics* **34**, 1-20.
- Menegotto, M. and Pinto, P. (1973). Methods of analysis for cyclically loaded R/C frames. *Symposium of Resistance and Ultimate Deformability of Structure Acted by Well Defined Repeated Load*, Lisbon, Portugal.
- Naeim, F. and Kelly, J.M. (1999). Design of Seismic Isolated Structures, Wiley: New York.
- OpenSees (2010). Open system for earthquake engineering simulation. Computer Program, University of California, Berkeley. Available from: <http://opensees.berkeley.edu>.
- PEER (2011). Pacific Earthquake Engineering Research Center Ground Motion Database. Available from: [http://peer.berkeley.edu/peer\\_ground\\_motion\\_database](http://peer.berkeley.edu/peer_ground_motion_database).
- Pant, D.R., Wijeyewickrema, A.C., and Ohmachi, T. (2010). Three dimensional nonlinear analysis of seismic pounding between multi-story reinforced concrete buildings. *Seventh International Conference on Urban Earthquake Engineering (7CUEE) and Fifth International Conference on Earthquake Engineering (5ICEE)*, Tokyo, Japan, 1829-1840.
- Pant, D.R. and Wijeyewickrema, A.C. (2012). Structural performance of a base-isolated reinforced concrete building subjected to seismic pounding. *Earthquake Engineering and Structural Dynamics* (in press).
- Park, R., Priestley, M.J.N., and Gill, W.D. (1982). Ductility of square-confined concrete columns. *Journal of Structural Engineering* (ASCE) **108**, 929-950.
- Pavlou, E.A. (2005). Performance of primary and secondary systems in buildings with seismic protective systems. *Ph.D. Dissertation*, State University of New York at Buffalo.
- Polycarpou, P.C. and Komodromos, P. (2010). On poundings of a seismically isolated building with adjacent structures during strong earthquakes. *Earthquake Engineering and Structural Dynamics* **39**, 933-940.
- Tsai, H.C. (1997). Dynamic analysis of base-isolated shear beams bumping against stops. *Earthquake Engineering and Structural Dynamics* **26**, 515-528.
- Yassin, M.H.M. (1994). Nonlinear analysis of prestressed concrete structures under monotonic and cyclic loads. *Ph.D. Dissertation*, University of California, Berkeley.